 DOI: 10.1002/masy.201100047

Photo-Crosslinkable Poly(trimethylene carbonate)-Based Macromers for Closure of Ruptured Intervertebral Discs

Shahriar Sharifi,[1] *Hendrik-Jan C. Kranenburg,*[2] *Björn P. Meij,*[2] *Dirk W. Grijpma**[1,3]

Summary: In patients with low back pain, surgical removal of the partially herniated nucleus pulposus may lead to clinical improvement but ultimately leads to intervertebral disc degeneration and recurrence of back pain is frequent. As an alternative treatment, use of an injectable material which solidifies *in situ*, is proposed. Such materials can easily fill oddly-shaped defects in the annulus fibrosus and seal the disc through a minimally invasive surgical procedure, thereby protecting the disc from further degeneration. In this study, a series of injectable and photo-crosslinkable macromers based on poly trimethylene carbonate (PTMC) and polyethylene glycol (PEG) were prepared. It is shown that these materials are injectable and solidify within two minutes upon illumination with visible light. By varying the PTMC to PEG block ratios, material properties such as elastic modulus and water content could easily be tuned to match those of the native annulus fibrosus. Ex vivo results using canine cadaveric spines showed the potential of the materials to seal an opening in the annulus fibrosus, although the adhesion of the photo-crosslinked material to the disc tissue needs to be improved.

Keywords: annulus fibrosus; injectable; intervertebral disc; low back pain; photopolymerization; poly(trimethylene carbonate)-based macromer

Introduction

Low back pain (LBP) is a major medical problem of immense socio-economical concern.[1–4] One of the main causes of LBP is degenerative disc disease (DDD) characterized by partial herniation of the nucleus pulposus (NP) through a ruptured annulus fibrosus (AF). This will eventually lead to intervertebral disc degeneration (IVDD).[5] Currently, removing the partially herniated NP and suturing the AF is the gold standard for treatment of DDD. Despite the fact that new emerging suturing techniques for annular closure are promising, disc reconstruction is usually not performed during these surgical procedures. Progressive IVDD may lead to structural failure of the IVD and AF prolapse at the original site of injury, *i.e.* where the annular structure has been disrupted, with recurrence of LBP.[6] Therefore, there is a great need for improved techniques and devices to repair annular defects at the moment of NP removal and prevent progressive IVDD and recurrent LBP.

Recent efforts have focused on tissue engineering strategies. A number of scaffolds have been suggested for AF tissue engineering, including collagen and hyaluronan,[7] chitosan,[8] aligned electrospun poly(ε-caprolactone) (PCL) fibers,[9] poly(1,8-octanediol malate),[10] polyglycolic

[1] Department of Biomedical Engineering, University Medical Centre Groningen, Antonius Deusinglaan 1, 9713 AV Groningen, The Netherlands
E-mail: d.w.grijpma@med.umcg.nl
[2] Department of Clinical Sciences of Companion Animals, Faculty of Veterinary Medicine, Utrecht University, PO Box 80154, 3508 TD Utrecht, The Netherlands
[3] MIRA Institute for Biomedical Technology and Technical Medicine, Department of Biomaterials Science and Technology, University of Twente, PO Box 217, 7500 AE Enschede, The Netherlands

acid meshes[11] and RGD-modified porous silk.[12] While many of these materials show promise, they need to be implanted as a replacement patch into the injured or diseased AF that requires invasive surgery. In addition, only few studies have addressed the need for fixing the implanted material within the annular defect.[13] Furthermore, tissue engineering attempts aim at regenerating AF tissue in the long term. Providing immediate mechanical strength after surgery is often neglected in these studies.

In this study, we hypothesized that minimally invasive injection of a biodegradable material into the torn AF and subsequent curing, not only can restore IVD function in the short term through immediate securing of disc material, but can also promote disc regeneration in longer times through degradation of the material and subsequent cellular infiltration. An ideal *in situ*-forming AF material should be readily injectable, easily infiltrate in surrounding tissue, and cure rapidly. The formed implant should have physical and mechanical properties that are close to those of AF tissue, and thereby not interfere with the restoration of the biomechanical properties of the disc. To develop an injectable system which meets the above requirements, we first focused on the synthesis of liquid triblock copolymeric macromers with three structural moieties: hydrophilic PEG that provides hydrophilicity, flexibility and allows wetting of the tissue;[14] oligomeric trimethylene carbonate (TMC) blocks that provide the elasticity and (enzymatic) degradability of the material;[15] and photo-crosslinkable methacrylate end groups which allow (photo)crosslinking.[16] In the next step, the developed systems were characterized in terms of their injecctability, curing and solidification time, and their physical and mechanical properties. To illustrate the potential of this injectable system as an AF sealant or restoration device, *ex vivo* experiments were conducted using canine cadaveric spines.

Experimental Part

Materials

Trimethylene carbonate (TMC) was purchased from Boehringer Ingelheim (Germany) and used without further purification. Stannous octoate (tin 2-ethylhexanoate, SnOct2), 1,6-hexanediol (99%) (HD), polyethylene glycol (PEG) (200, 600 and 1000 $g \cdot mol^{-1}$), triethyl amine (TEA), methacrylic anhydride (MA), camphorquinone (CQ) photoinitiator, N,N-Dimethyl-p-Toluidine (DMPT) and hydroquinone were purchased from Sigma-Aldrich (U.S.A.) and used as received. Analytical grade dichloromethane (DCM) was obtained from Biosolve (The Netherlands). DCM and toluene were dried over CaH_2 and distilled. The PEG were dried by azeotropic distillation with toluene. Other solvents (Biosolve, The Netherlands) were of technical grade and were used as received.

Synthesis and Characterization of Macromers

Poly(trimethylene carbonate) (block co) oligomers were first synthesized by ring opening polymerization of trimethylene carbonate in the presence of HD, PEG200, PEG600 or PEG1000 as initiator. A typical procedure for the preparation was as follows: TMC, initiator and $Sn(Oct)_2$ (0.2 mmol/per mol monomer) as catalyst were reacted in the melt at 130 °C for 72 h under argon atmosphere. Oligomers with a targeted molecular weight of approximately 2000 $g \cdot mol^{-1}$ were prepared by adjusting the initiator to monomer ratios.

The synthesized oligomers were subsequently methacrylate-endcapped using methacrylic anhydride in the presence of triethyl amine. The (co) oligomers first were dissolved in DCM and MA and TEA (4 mol/mol oligomer) and charged into a three-necked round bottom flask under argon atmosphere. The reaction was allowed to proceed for 72 h at room temperature. Then, 200 ppm hydroquinone was added to the solutions and the macromers were purified by removal of the formed methacrylic acid and the excess

methacrylic anhydride by vacuum distillation at 120 °C. The macromers were then dissolved in DCM and precipitated in excess cold hexane. The macromers were dried in a vacuum oven at 30 °C for 24 h and stored at −20 °C until use. The oligomer syntheses and the functionalization reactions are schematically shown in Figure 1. The macromers are labeled as MA-PTMC-*initiator*-PTMC-MA, in which *initiator* is HD or the corresponding PEG. For example, MA-PTMC-PEG200-PTMC-MA macromers are prepared using PEG of molecular weight of 200 $g \cdot mol^{-1}$ as the initiator.

Macromer molecular weights and degrees of functionalization were determined by ^{1}H-NMR spectroscopy (Varian Innova 300 MHz, USA), using $CDCl_3$ (Merck, Germany) as the solvent. The thermal properties of the macromers were assessed by differential scanning calorimetry (DSC) employing a Perkin Elmer Pyris 1 (USA). To erase the thermal history of the samples, 5–10 mg samples were heated from −100 °C to 100 °C at a heating rate of 10 °C/min and quenched rapidly (300 °C/min) to −100 °C. After 5 min, a second scan was recorded. In second run the glass transition temperature, T_g, was taken as the midpoint of the heat capacity change, the melting point (T_m) was determined as the maximum of the endothermic peak. The viscosity of macromers was determined at room temperature using a US 200 rheometer (Anton Paar, Austria). The experimental settings were a flat plate geometry (25 mm diameter, 0.5 mm gap), a strain of 1% and a frequency of 1 Hz.

Photo-Crosslinking Kinetics by Fourier Transform Infrared (FTIR) Spectroscopy

Fourier Transform Infrared Spectroscopy (FTIR) experiments (4000–600 cm^{-1}) using a Perkin-Elmer Spectrum 1000 FTIR spectrometer (USA) at 4 cm^{-1} resolution were performed at room temperature for investigation of the curing kinetics. An amount of macromer was dissolved in dry DCM, and CQ (2 wt% of the macromer) was added. 100 μl of this solution was then cast on a KBr disc and left in the dark in a vacuum oven for 4 h to evaporate the solvent. A spectrum of the non-crosslinked material was then collected. With use of a light probe (Optilux 501, USA, 10 mm diameter light probe, 470 nm blue light) the specimens were illuminated for 10 s with an intensity of 200 mW/cm^2). Immediately after light exposure, a second spectrum was collected. This process was repeated until the samples were illuminated for a total time of 280 s. The C=C stretching vibrations at 1670–1600 cm^{-1} were used as characteristic infrared absorbance bands to monitor the conversion of the methacrylate double bonds during photo-crosslinking. The area of these peaks was integrated and normalized to the peak area of the carbonyl (C−O) peak at 1730 cm^{-1} to correct for polymerization shrinkage during

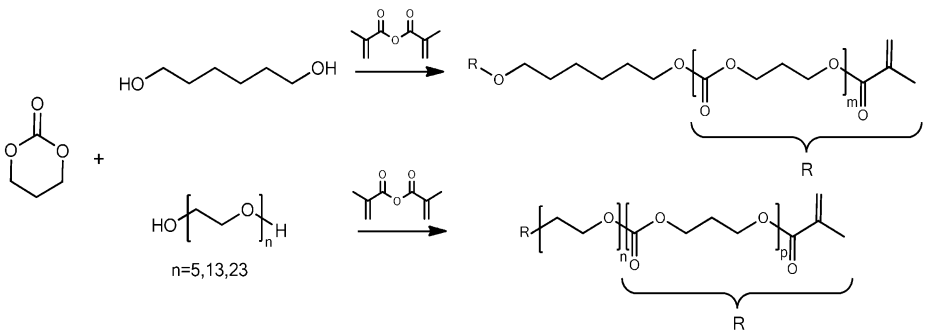

Figure 1.
Schematic route employed to synthesize PTMC and PTMC-PEG-PTMC macromers.

the reaction. The conversion was calculated from the decrease of the peak area in time:

$$Conversion\,(t) = \frac{A_{t=0} - A_t}{A_{t=0}} \times 100 \qquad (1)$$

Here $A_{t=0}$ is the peak area of the C=C bonds at the beginning of the reaction (non-irradiated specimens, $t = 0$) and A_t is the peak area at illumination time t. To check if crosslinking continued in the dark, double bond conversions were also determined after different time periods after the illumination. The photo-crosslinking rates were determined by numerical differentiation from the double bond conversion versus time data.

To investigate the effect of a tertiary amine on the photo-crosslinking kinetics, DMPT (0.08 wt% with respect to the macromer) was added to the macromer and CQ solutions in DCM.

Preparation of PTMC-Based Networks by Photo-Crosslinking and Characterization

PTMC-based networks were prepared by photo-crosslinking Optilux 501 apparatus with a blue light intensity of circa $200\,mW \cdot cm^{-2}$ using CQ/DMPT as photo-initiating system. Typically, CQ (2 wt% with respect to the macromer) was first dissolved in the macromer, after which DMPT (0.08 wt % with respect to macromer) was added. The mixtures were cast in metal molds and cured for 200 s to give discs with a diameter of 6 mm and a height of 3 mm.

The gel content of the photo-crosslinked specimens were determined by swelling in DCM. The as-prepared samples were first weighed (w_i) and then immersed in excess of DCM. After 72 h, the specimens were dried in a vacuum oven for 36 hrs (at 40 °C), and their dry

$$Gel\,fraction\,(\%) = 100 - \frac{w_i - wi_d}{w_i} \times 100 \qquad (2)$$

Water-uptake measurements were also conducted. As-prepared samples were immersed in excess distilled water until constant weight was reached (w_w). Then the specimens were dried in a vacuum oven at 70 °C for 72 h and weighed (w_d). Water-uptake was calculated using:

$$Water\,uptake\,(\%) = \frac{w_w - w_d}{w_d} \times 100 \qquad (3)$$

The thermal properties of the networks in the dry- as well as in the wet state after equilibration in water were evaluated by DSC as described before, by quenching to −50 °C and heating to 30 °C at 10 °C/min. In the wet specimens, the fraction of freezable and non-freezable (bound) water could be determined as described by Wang *et al.*[17]

The elastic modulus (E) of the photo-crosslinked PTMC-based networks in the dry and in the wet state were determined at room temperature in compression using a Zwick Z020 tensile tester (Germany) equipped with a 500 N load cell. Photo-crosslinked discs (with a diameter of 6 mm and a height of 3 mm in the dry state) were compressed at a rate of 30% per min. The value of E was determined from the slope of the linear region in the compressive stress-strain curves.

The depth of cure of the macromers was determined in a manner similar to that described in ISO 4049. The mixtures of macromer and initiating system were inserted into a cylindrical mold (10 mm length and 6 mm internal diameter), covered with glass slides and irradiated for 200 s with blue light as described above. Non-cured material was carefully removed with a plastic spatula, and the length of the cured cylinder was equated to the depth of cure.

Cross-Linking of PTMC-Based Macromers in Cadaveric Canine Intervertebral Discs

The potential of using the macromers as an injectable AF closure device was evaluated using canine cadaveric discs. The lumbar spines of beagle dogs were immediately frozen at −20 °C after euthanization. Prior to use, the spines were left to thaw for 24 hours at room temperature. Excess muscle was removed, but ligamentous tissue was left intact. Before application

Table 1.
Locations of the IVDs in the canine cadaveric spines into which the different macromers were injected and subsequently photo-crosslinked.

Macromer	IVD in cadaveric canine spine[a]
MA-PTMC-HD-PTMC-MA	L5-L6, T13-L1
MA-PTMC-PEG200-PTMC-MA	L5-L6, T13-L1
MA-PTMC-PEG600-PTMC-MA	L3-L4, L2-L3
MA-PTMC-PEG1000-PTMC-MA	L1-L2, L4-L5

[a]L and T stand for the lumbar and thoracic vertebrae, respectively. L5-L6 for example indicates the disc between the L5 and L6 vertebrae.

of the macromers, a nuclectomy of the lumbar IVDs was performed after making a stab incision in the AF via a left lateral approach to the IVD. This is approach is similar to the surgical procedure done in human and canine DDD patients.[18] An incision was made in the transverse midline of the IVD, parallel to the fibers of the outer annular ring using a surgical blade nr 11. The NP was removed with ball-tipped probes and a grasping forceps.

Then the macromers mixed with the CQ/DMPT initiating system (concentrations are as described before), were injected into and on the AF defect area using a syringe equipped with a gage 18 needle. The macromer mixtures were exposed to blue light for 200 s. The injections were done in IVDs at different locations of the spine, as is listed in Table 1. After closing of the annular defects upon injection and curing of the macromers, the spines were placed in an incubator overnight at 37 °C. The IVDs were carefully transected, and the infiltration of the macromer in the disc tissue, the extent of cross-linking and the efficiency of closing the annular defects was evaluated.

Results and Discussion

Synthesis and Characterization of PTMC-Based Macromers

A series of TMC-based macromers, varying in chemical composition and physical characteristics, were prepared by ring opening (co)polymerization of TMC in the presence of low molecular weight PEGs (with Mn values of 200, 600 or 1000 $g \cdot mol^{-1}$) or hexanediol as initiating species. The hydroxyl group terminated oligomers were end-functionalized by reaction with methacrylic anhydride.

The structure and the M_n values of the (triblock) macromers were determined by ^{1}H-NMR (Table 2). The TMC block lengths and the total molecular weights of the macromers were close to the intended values (2000 $g \cdot mol^{-1}$), as could be determined from the TMC to PEG integral ratios in the NMR spectra. In the spectra, the TMC ($-COOCH_2CH_2CH_2O-$) resonances are at 4.1–4.3 ppm, while the PEG resonances ($-O-CH_2-CH_2-$) occur at 3.5–3.7 ppm. For the MA-PTMC-Hexanediol-PTMC-MA macromer, the M_n values were calculated from the peak integrals of the HD resonances ($-CH_2-$, 1.35–1.44 ppm) and those of TMC (4.1–4.3 ppm). For all macromers, TMC conversion was more than 98%.

The degree of functionalization of the macromers was calculated from the integral ratios of the methacrylate $-CH=CH_2$ protons at 5.6–6.4 ppm to the PEG protons ($-O-CH_2-CH_2-$) at 3.5–3.7 ppm or to the HD protons at 1.34–1.44 ppm. As shown in Table 2, the degree of functionalization of the macromers was higher than 95%. It

Table 2.
Characteristics of the different synthesized PTMC-based macromers.

Macromer	M_n ($g \cdot mol^{-1}$)	TMC[a] (mol%)	DF[b] (%)	T_g (°C)	*Viscosity (Pa.s)*
MA-PTMC-PEG(200)-PTMC-MA	1875	94	95	−51.1	990
MA-PTMC-PEG(600)-PTMC-MA	1820	92	98	−49.4	13.2
MA-PTMC-PEG(1000)-PTMC-MA	1900	89	98	−53.2	6.16
MA-PTMC-Hexanediol-PTMC-MA	2050	94	98	−43.7	90.0

[a]TMC content in the macromer (in mol %).
[b]Degree of functionalization with methacrylate end groups.

should be noted that terminal hydroxyl terminal groups could not be discerned in ^{1}H-NMR spectra, also suggesting that the functionalization reaction was essentially complete.

The thermal characteristics of the synthesized macromers as determined by DSC are shown in Table 2. All macromers had low (single) glass transition temperatures ranging from −43 to −53 °C. Only the MA-PTMC-PEG(1000)-PTMC-MA macromer was crystallizable with a melting point of the PEG component of 22 °C and a crystallinity of 8%. This latter value is determined from the heat of fusion $\Delta H_m = 205.8$ J/g for fully crystalline PEG.[19] Before block copolymerization with TMC, the melting temperature of the PEG and its crystallinity were respectively 37 °C and 61%. The attachment of TMC to the ends of PEG chains hinders the crystallization of PEG. This behavior is similar to that observed for other PEG triblock copolymers reported in the literature.[20,21]

While the glass transition temperatures of the macromers did not depend on composition, the viscosity of the macromers decreased with increasing PEG block molecular weight (and decreasing TMC content).

Photo-Crosslinking Kinetics by Fourier Transforms Infrared (FTIR) Spectroscopy

As the objective of this study was to develop an *in situ* photo-crosslinkable

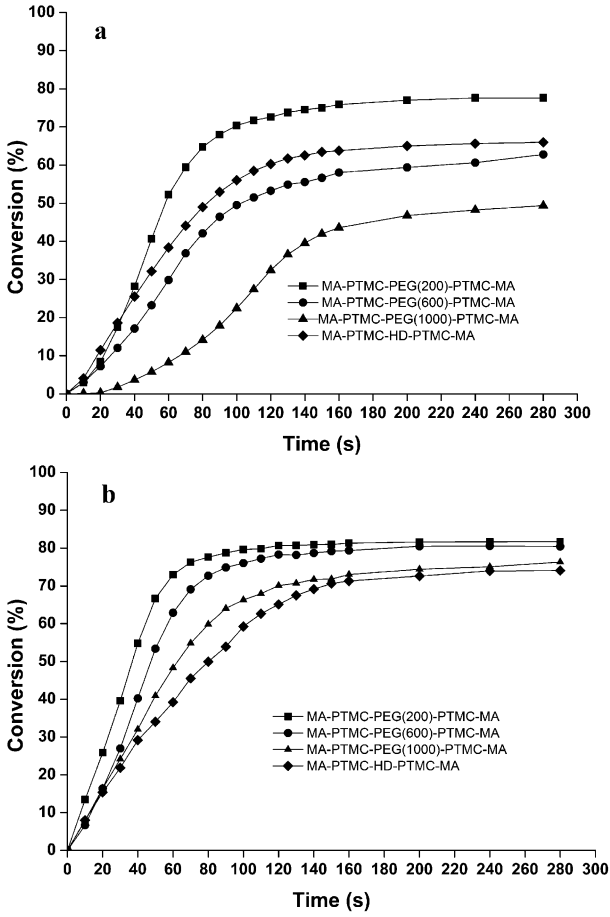

Figure 2.
Photo-crosslinking kinetics of the different PTMC-based macromers as determined by FTIR, showing the effect of the initiating system. a) CQ photo-initiator; b) CQ with DMPT as the photo-initiating system.

annular closure device, whereby a solid network forms within minutes, the kinetics of the macromer double bond conversion upon illumination with blue light in the presence of CQ need to be investigated. Although CQ alone can be an effective initiator in some systems, the hydrogen abstraction reaction of triplet $^3CQ^*$ with amines such as DMPT to generate free radicals proceeds much more rapidly.[22,23]

In Figure 2, the photo-crosslinking kinetics of the macromers, as determined by following the double bond conversion by FTIR in time, are shown. Several steps in the photo-polymerization are noticeable from the shape of the conversion curves, these are autoacceleration, autodeceleration and a limiting maximal conversion of the functional groups (81%).[24] In the dark, in the absence of further radical initiation, photo-polymerization is minimal as the rate of polymerization declines rapidly.

Photo-polymerization rates are highest at double bond conversions of 20 to 40%, in agreement with the literature.[25] Although the molecular weight of the different macromers was very similar, and consequently the concentration of double bonds as well, the polymerization rates varied with macromer structure and composition, see the data presented in Figure 2 and Table 3. It has been shown that monomer structure, composition of the macromer system, oxygen concentration and temperature can affect the kinetics of the polymerization.[25]

In our case, increasing the PEG content of the macromers decreased the maximal polymerization rates ($R_p$max). The maximal reaction rate can be an indication of the magnitude of the gel effect. With decreasing PEG contents of the macromers, their viscosities increase (see Table 2). High viscosities result in increased polymerization rates due to a decrease in mobility of the macroradical chain ends and decreased termination rates.[26] In addition, it has been shown that at high concentration of ether groups, hydrogen abstraction from these groups can compete with the addition of an initiator radical to the monomer, thereby slowing down the polymerization.[27]

With only CQ as photoinitiator (Figure 2a), maximal conversion and polymerization rates were relatively low. The lowest conversions were reached for MA-PTMC-PEG(1000)-PTMC-MA, with only 50% conversion after 280 s illumination. The other macromers, with lower PEG contents, reached somewhat higher maximal conversions of 62 to 77%. These poor conversions are due to vitrification of the polymerizing systems, where especially at low conversion rates diffusion of the radicals is limited. The extent of double bond conversion is low even after long illumination times. The macromer double bond conversion curves shown in Figure 2b and the data presented in Table 3 indicate that in the presence of DMPT for all macromers polymerization rates and maximal conversions are significantly higher than in the absences of DMPT. After 280 s illumination, the macromers now reached maximal double bond conversion (DC) of 74 to 80%.

It can be concluded that although the concentration of radicals produced by

Table 3.
Maximal methacrylate double bond conversion rates and corresponding double bond conversions (DC) in the photo-crosslinking of PTMC-based macromers. Photo-initiation is done using CQ in the absence or presence of DMPT.

Macromer	$R_p$max (%/s) Initiator		DC at $R_p$max(%) Initiator	
	CQ	CQ/DMPT	CQ	CQ/DMPT
MA-PTMC-PEG(200)-PTMC-MA	1.24	1.50	29	41
MA-PTMC-PEG(600)-PTMC-MA	0.70	1.30	28	40
MA-PTMC-PEG(1000)-PTMC-MA	0.49	0.88	27	37
MA-PTMC-Hexanediol-PTMC-MA	0.74	0.73	4.6	21

hydrogen abstraction from macromers using only CQ is sufficient to initiate radical polymerization, use of a CQ/DMPT initiating system is significantly more efficient.

Preparation of PTMC-Based Networks by Photo-Crosslinking and Characterization

To obtain PTMC-based networks with physical properties that match those of AF tissue, networks were prepared by photo-crosslinking of PTMC-based macromers containing varying amounts of PEG using a CQ/DMPT photo-initiating system. In Table 4, the characteristics of the different (disc-shaped) networks prepared in molds are summarized. These include important network properties such as gel fraction, water uptake and thermal properties, as well as the depth of cure of the systems that can be reached in our experiments.

The gel content of all networks was high (close to 90%) after 200 s of photo-polymerization. After crosslinking, all networks were amorphous (also in the case of MA-PTMC-PEG(1000)-PTMC-MA), where the presence of cross-linkages inhibits crystallization). Furthermore, it can be seen in the table that compared to the T_g of the starting materials, T_g of the networks had significantly increased upon crosslinking. This is due to the restricted the mobility of the chain segments.

The uptake of water by the different networks strongly depends on composition. While MA-PTMC-Hexanediol-PTMC-MA networks were quite hydrophobic and did not absorb significant amounts of water, networks containing PEG were quite hydrophilic. In these cases water uptake by the networks increased with increasing amount of PEG. The water contents of these networks were comparable to that of the annulus fibrosus (60–70%), indicating their compatibility with AF tissue.[28] The table also shows that in the hydrated MA-PTMC-PEG(200)-PTMC-MA and MA-PTMC-PEG(600)-PTMC-MA networks, most of the water is bound water. This water is likely oriented by hydrogen bonding to the ether groups of the PEG component in the network. For MA-PTMC-PEG(1000)-PTMC-MA networks the total uptake and content of water is much increased, the fraction of non-bonded (free or bulk) water is much higher. This can be important as the physical state of the absorbed water can determine the interaction between the hydrated network and proteins present in tissues, and thereby influencing reactivity and biocompatibility of the networks.

For our intended application, where the materials are first injected and subsequently photo-polymerized in the tissue, the depth of cure of the macromers is of interest. For the different macromers the depth of cure with the CQ/DMPT initiating system was more than 7 mm in all cases, which is quite sufficient. This high depth of cure achieved by visible light curing using CQ is due to its photobleaching characteristics and due to the fact that visible light is not absorbed by most organic compounds.[29]

The values of the elastic modulus of the amorphous PTMC-based networks measured in compression are shown in Figure 3. In the dry state, the networks prepared from MA-PTMC-PEG(200)-PTMC-MA had the highest modulus of 19.4 MPa. With increasing PEG content, the elastic modulus decreased and a value of 5.5 MPa was found for networks prepared from MA-PTMC-PEG(1000)-PTMC-MA.

Table 4.
Physical properties of PTMC-based networks prepared by photo-crosslinking with a CQ/DMPT initiating system in molds.

Material	Gel fraction (%)	T_g (°C)	Water uptake (%)	Bound water (%)	Cure depth (mm)
MA-PTMC-PEG(200)-PTMC-MA	90 ± 1.2	−9.4	6.3 ± 0.8	4	8 ± 0.3
MA-PTMC-PEG(600)-PTMC-MA	87 ± 1.8	−17.7	18.8 ± 0.5	16	8 ± 0.4
MA-PTMC-PEG(1000)-PTMC-MA	90 ± 0.5	−23.0	54.5 ± 1.0	32	7.5 ± 0.2
MA-PTMC-Hexanediol-PTMC-MA	88 ± 2	−9.7	1.0 ± 0.2	0.002	9 ± 0.5

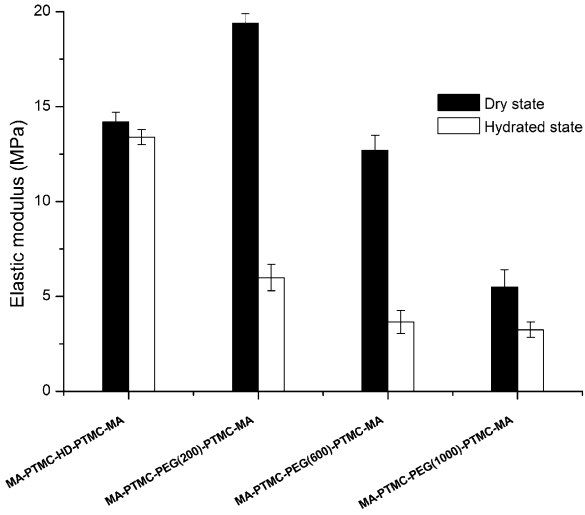

Figure 3.
Elastic modulus values determined in compression of PTMC-based networks in the dry sate and in the wet hydrated state. The different networks take up different amounts of water, see Table 4.

This reduction can be attributed to the presence of ether bonds in the polymer backbone which can lead to increased flexibility of the material. Furthermore, as previously discussed, the lower conversion of macromers containing the highest amounts of PEG could have resulted in a higher amount of non-elastically active chains and reduced crosslinking densities. Reduced crosslinking densities can result in lower elastic modulus values.

After equilibration in water, the elastic modulus of the hydrated networks decreased significantly. PTMC-based networks with the highest amounts of PEG take up the most water, and concomitantly have the lowest modulus values in the wet state.

Networks prepared using MA-PTMC-HD-PTMC-MA had relatively high E modulus values. As these networks take up only limited amounts of water, the rigidity did not change much upon equilibration in water.

The annulus fibrosus is a heterogenic tissue, with an elastic modulus of 5 to 40 MPa depending on the anatomical location.[30] The determined elastic modulus values of the PTMC-based networks indicate that the mechanical properties of these materials should be adequate to use in functional repair of damaged AF tissue.

Photo-Crosslinkable PTMC-Based Macromers as Annulus Closure Devices

The wetting of canine cadaveric IVD tissue by the different liquid PTMC-based macromers was first evaluated qualitatively. All macromers were found to spread well on the surface of the tissue, showing good adherence. The contact angles of the PEG-containing macromers on IVD surfaces were around 40°, as was roughly estimated from microscopy images after putting a drop of the macromers on the IVD tissue. The contact angle of the MA-PTMC-HD-PTMC-MA macromer had a slightly higher contact angle of around 45°, which correlates with the low hydrophilicity of the macromer.

At room temperature, all macromers could readily be injected through an 18 gauge needle. Figure 4a shows the manner in which the macromers are injected into the nucletomized canine cadaveric intervertebral disc. By illumination of the macromers through the annular defect with blue light for 200s, shown in Figure 4b, a network is formed with the intervertebral disc. In Figure 4c and 4d are photographic

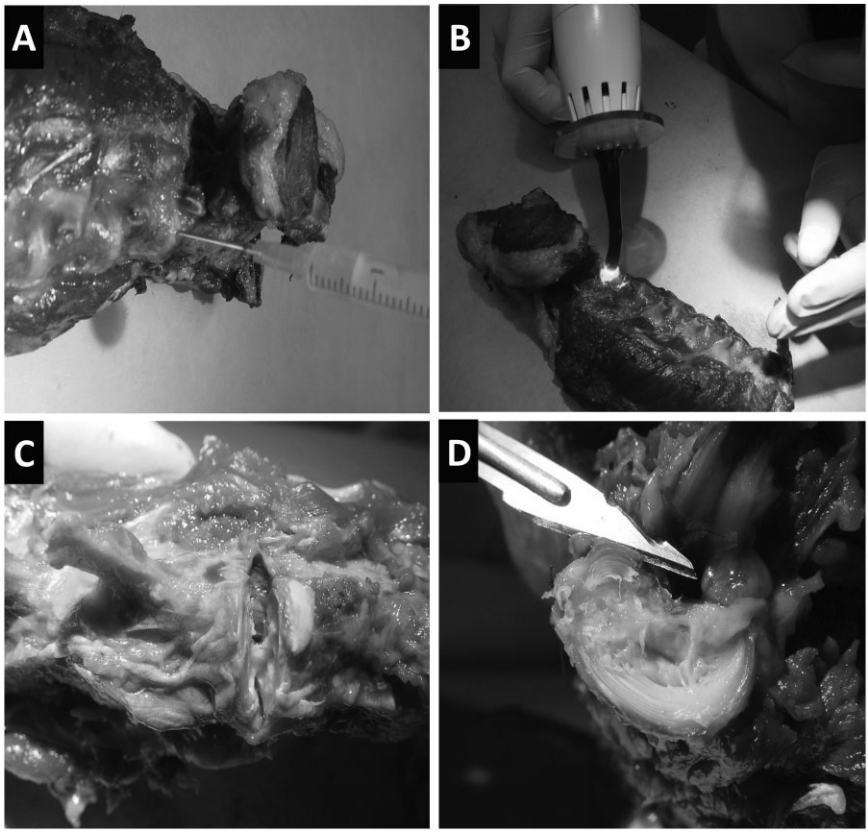

Figure 4.
Injection of a curable (MA-PTMC-PEG(200)-PTMC-MA) resin formulation into a nucletomized canine cadaveric intervertebral disc (A). In situ photocuring of the macromer with blue light (B). Dissected intervertebral disc after photocuring of the PTMC-based macromer (C). Photocrosslinked PTMC-based network in the nucletomized intervertebral disc (D).

images of the dissected canine cadaveric intervertebral discs in which the photo-crosslinked PTMC-based network is present.

The depths of cure determined in cylindrical molds was 7 mm or more, as described before, and it was to be expected that this would be to be more than sufficient to allow photo-crosslinking in situ. Upon examination of the discs after dissection, it was indeed found that the macromers could be cured to form a flexible and elastic network within the intervertebral disc cavity. In some cases, however, the nucletomized intervertebral discs were not completely filled; it is likely that the internal pressure within the intervertebral disc had made it difficult to completely fill the cavity with resin. It was also found that cross-linking was less efficient in the IVD cavity than in the cylindrical molds used to determine the depth of cure. With exception of the resins based on the MA-PTMC-PEG(200)-PTMC-MA macromer, the extent of double bond conversion and network formation, as could quantitatively be assessed from the stickiness of the networks, seemed to be lower. This reduced rate of curing can be due to blockage of the pathway of the light, or due to dilution of macromer resin compositions in the aqueous environment of the intervertebral disc.

Of the resins that were fully cured *in situ*, the strength of adhesion to the interverteb-

ral disc tissue was qualitatively assessed. It was found that while the non-crosslinked macromer resins showed excellent spreading and adhesion to the tissue, the attachment of the cured PTMC-based networks to the tissue was not very strong. Although there was attachment to some extent, it is not sure if adhesion would be strong enough to prevent detachment to or expulsion from the IVD in clinical use.

Conclusion

The results presented in this study show that PTMC-based macromer formulations can be injected and photo-crosslinked *in situ* in a nucletomized intervertebral disc. By preparing block copolymeric macromers with different contents of PEG and TMC, biodegradable network materials with varying properties can be prepared. Important physical properties such as elastic modulus and hydrophilicity can be optimized to match those of native AF tissue. Studies in canine cadaveric spines showed that, while the depth of cure in the intervertebral disc cavity is sufficient to achieve adequate network formation, the adhesion of the photo-crosslinked materials to the disc tissue might need to be enhanced.

Acknowledgements: This research forms part of the Project P2.01 IDiDAS of the research program of the BioMedical Materials institute, co-funded by the Dutch Ministry of Economic Affairs, Agriculture and Innovation.

[1] B. G. Druss, S. C. Marcus, M. Olfson, H. A. Pincus, *Health Affairs* **2002**, *21*, 105.
[2] J. W. Frymoyer, W. L. Cats-Baril, *Orthop Clin North Am* **1991**, *22*, 263.
[3] T. S. Carey, J. M. Garrett, A. Jackman, N. Hadler, *Med Care* **1999**, *37*, 57.
[4] G. B. Andersson, *Lancet* **1999**, *354*, 581.
[5] M. A. Adams, P. J. Roughley, *Spine* **2006**, *31*, 2151.
[6] E. W. Fritsch, J. Heisel, S. Rupp, *Spine* **1996**, *21*, 626.
[7] M. Alini, W. Li, P. Markovic, M. Aebi, R. C. Spiro, P. J. Roughley, *Spine* **2003**, *28*, 446.
[8] P. Roughley, C. Hoemann, E. DesRosiers, F. Mwale, J. Antoniou, M. Alini, *Biomaterials* **2006**, *27*, 388.
[9] N. L. Nerurkar, B. M. Baker, S. Sen, E. E. Wible, D. M. Elliott, R. L. Mauck, *Nat Mater* **2009**, *8*, 986.
[10] Y. Wan, G. Feng, F. H. Shen, G. Balian, C. T. Laurencin, X. Li, *Macromol Biosci* **2007**, *7*, 1217.
[11] H. Mizuno, A. K. Roy, C. A. Vacanti, K. Kojima, M. Ueda, L. J. Bonassar, *Spine* **2004**, *29*, 1290.
[12] G. Chang, H. J. Kim, G. Vunjak-Novakovic, D. L. Kaplan, R. Kandel, *J Biomed Mater Res A* **2010**, *92*, 43.
[13] J. C. Iatridis, R. M. Schek, A. J. Michalek, *European Cells & Materials* **2011**, *21*, 373.
[14] H. Kobayashi, S. H. Hyon, Y. Ikada, *J Biomedl Mater Res* **1991**, *25*, 1481.
[15] E. Bat, T. G. van Kooten, J. Feijen, D. W. Grijpma, *Biomaterials* **2009**, *30*, 3652.
[16] T. Matsuda, I. K. Kwon, S. Kidoaki, *Biomacromolecules* **2004**, *5*, 295.
[17] S. Gunasekaran, T. Wang, *J Appl Polym Sci* **2006**, *101*, 3227.
[18] R. Bertagnoli, R. J. Vazquez, *J Spinal Disord Tech* **2003**, *16*, 398.
[19] S. F. Wang, L. C. Lu, J. A. Gruetzmacher, B. L. Currier, M. J. Yaszemski, *Biomaterials* **2006**, *27*, 832.
[20] I. Rashkov, N. Manolova, S. M. Li, J. L. Espartero, M. Vert, *Macromolecules* **1996**, *29*, 50.
[21] T. Kissel, Y. X. Li, F. Unger, *Adv Drug Deliv Rev* **2002**, *54*, 99.
[22] J. Jakubiak, X. Allonas, J. P. Fouassier, A. Sionkowska, E. Andrzejewska, L. Å. Linden, J. F. Rabek, *Polymer* **2003**, *44*, 5219.
[23] S. Sharifi, M. Imani, H. Mirzadeh, M. Atai, F. Ziaee, R. Bakhshi, *J Biomed Mater Res Part A* **2009**, *90A*, 830.
[24] K. S. Anseth, C. Decker, C. N. Bowman, *Macromolecules*, **1995**, *28*, 4040.
[25] E. Andrzejewska, *Progr Polym Sci* **2001**, *26*, 605.
[26] E. Andrzejewska, A. Marcinkowska, *J Appl Polym Sci* **2010**, *116*, 280.
[27] S. Davidson, *Exploring the science, technology and applications of UV and EB curing*, SITA Technology Limited, London **1999**.
[28] N. L. Marinelli, V. M. Haughton, A. Munoz, P. A. Anderson, *Spine* **2009**, *34*, 520.
[29] M. Imani, S. Sharifi, H. Mirzadeh, M. Atai, F. Ziaee, *J Biomed Mater Res Part A* **2008**, *84A*, 545.
[30] S. Ebara, J. C. Iatridis, L. A. Setton, R. J. Foster, V. C. Mow, M. Weidenbaum, *Spine* **1996**, *21*, 452.

